ACS OMEGA

Open Access

http://pubs.acs.org/journal/acsodf

Article

Adsorption of Bacteria Extracellular Polysaccharide Substances on the Graphite (002) Surface: A DFT and MD Study

G. Plason Zuerkanah Plakar,* Fredy Harcel Kamgang Djioko, Emeka Emmanuel Oguzie,* and Kanayo L. Oguzie

Cite This: *ACS Omega* 2024, 9, 48711−48720

Read Online

ACCESS | Metrics & More | Article Recommendations | Supporting Information

ABSTRACT: Understanding the principle of the bacteria−anode surface interaction can enhance electron transfer in microbial fuel cells and aid in antibiofouling. In this article, we investigate the adsorption propensity of common adhesins [*N*-acetylglucosamine (NAG), D-glucose, and alginate] found in microbial biofilms on the surface of unmodified and modified graphite through density functional theory and molecular dynamics simulations. DFT results showed that all the molecules could interact with the graphite surface, with NAG (ΔE_{gap} = 3.677 eV) being the most reactive molecule. The Fukui function results show that the most active sites were located at O, C_{13}, and N on the adsorbates. The optimum conditions were basic medium at 303 K across all systems. All adsorbates show energetically favorable adsorption, with NAG showing the maximum adsorption energy irrespective of the modification. The modified graphite system showed increased adsorption compared to the unmodified graphite system. Electrostatic interactions, H-bonding, and $\pi-\pi$ stacking or interactions are the driving forces responsible for the chemical bond formation in the adsorbates−adsorbent complexes. Altogether, this research provides theoretical support for bacterial adhesin adsorption onto graphite anodes and new ideas for studying bacteria−anode interactions in fuel cells, biofouling and antifouling, dental science, clean energy production, and wastewater treatment.

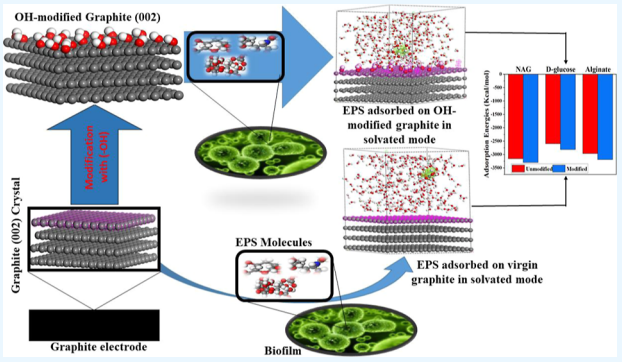

1. INTRODUCTION

The advancements in technology demand the availability of adequate electrical energy. Nonrenewable fossil fuels, including crude oil, natural gas, and coal, have been the source of electrical energy for decades. Despite their contribution, these fossil fuels are harmful, as they contribute to global warming, emit greenhouse gases, and accelerate climate change. As such, sources of green and renewable energy such as solar, wind, and hydro energy have received immense attention due to their potential to reduce greenhouse gases, improve the quality of our air, reduce climate change, and improve clean water access. However, these energy sources are intermittent and often require gross start-up costs. Therefore, there is a need for more reliable and clean energy technologies. Among these technologies, microbial fuel cells have attracted much attention due to their weather independence, utilization of cheap biomass feedstock to effortlessly produce bioelectricity while offering bioremediation, and ease of operation. They were first introduced in 1911 and have advanced rapidly. However, the performance of this technology to compete with the existing fossil fuels heavily relies on electrode performance. As a result, current research is developing new electrode materials, among which carbon-based electrode materials have attracted current research.[1]

Carbon-based electrode materials have attracted extensive research in recent times due to their applications in energy storage and conversion, water treatment, filtration and purification, environmental remediation, electronics, automotive engineering, and nanomaterials in fuel cell technology for sustainable energy production. These materials are famous for their high conductivity, thermal and chemical stability, biocompatibility, and mechanical strength.[2,3] Examples of some conventional carbon-based electrodes include carbon cloth, carbon paper, carbon fiber, carbon felt, graphitic carbon, and graphene-based nanocomposites.[4] With its atomically flat and chemically inert surface, graphite offers a well-defined model system for accommodating the adsorption of electrigens through their extracellular polysaccharide substances (EPSs).[5] A unique π-conjugated graphene method, the basic structural unit of graphite, can interact with functional groups present in EPS molecules through various mechanisms, including hydro-

Received: August 31, 2024
Revised: October 13, 2024
Accepted: October 17, 2024
Published: November 23, 2024

gen bonding, $\pi-\pi$ stacking, and van der Waals forces.[6] However, pristine graphitic surfaces exhibit limited functionality to effectively accommodate bacteria adsorption and therefore require modification to optimize their interaction with specific target molecules.[7] Since a better understanding of how well bacteria attach to the anode surface can influence the overall power output or antibiofouling of the anode and cathode, respectively, it therefore becomes imperative to tune into the molecular interaction between the bacteria and the anode surface. The low porosity and inadequate specific surface area (ssa) restrict the adhesion of bacteria, compelling scientists to perform surface modification as an improvement method.[8,9]

In one study, Collignon et al.[10] studied the interaction between small water molecules and hydroxylated graphite surfaces utilizing quantum calculations using the ONIOM approach by anchoring the −OH groups to the graphite surface. Their results show that the adsorption energies were higher for modified (or hydroxylated) graphite compared to those for the bare graphite surface. Hydroxylated graphite consists of C−O−H bonds covalently bonded in an sp3 hybridization.[10] Based on its improved biocompatibility, chemical stability, high electrical conductivity, and large surface area,[11] surface-modified graphite is postulated to be suitable for the adsorption of bacteria EPS, which are long, thin molecular chains produced by bacteria, ranging in mass from 0.5 to 2.0 × 10^6 Da. These EPS include *N*-acetyl-glucosamine (monomer of poly-*N*-acetyl-glucosamine, PNAG),[12] cellulose,[13] alginate,[14] and several others.[15] Poly-*N*-acetylglucosamine (NAG) is found mainly in *Staphylococcus aureus* and *Staphylococcus epidermidis* biofilms. Evidence shows that *S. aureus* and *S. epidermidis* use PNAG to attach to abiotic surfaces.[16] Abundantly available alginate in the biofilm of *Pseudomonas aeruginosa* functions in the stability and initial cell attachment, increasing both the rate and the extent of attachment.[14] Cellulose, mainly composed of β-D-glucose, is one of the most common EPS. The cellulose monomer contains a long β- (1, 4)-D-glucose chain, which enhances biofilm formation on certain biotic and abiotic surfaces when coexpressed with fimbriae.[17] Unarguably, a better understanding of the adsorption behavior of these EPS on electrode surfaces will enable the design of microbial bioelectrochemical systems with improved performance and functionality for electron transfer.

Previous studies have employed various wet chemistry techniques, such as atomic force microscopy (AFM)[17] and scanning probe microscopy[18] to investigate surface-attached biofilms. For instance, Wan Dagang et al.[19] compared the adhesion of pseudomonas fluorescence biofilms on stainless steel, glass, and cellulose using AFM imaging. The glass system attained the highest binding force (48 ± 7 nN), followed by stainless steel (30 ± 7 nN), while the lowest binding force was cellulose (7.8 ± 0.4 nN). Yang et al.[20] examined the stability of substrate-sorbate systems under different environmental conditions on EAK16-II-hydrophobic highly ordered pyrolytic graphite and EAK16−16-mica surfaces. Their result indicated that EAK16-II-modified mica surfaces are more stable in an acidic medium than in an alkaline solution, while the degree of coverage of modified HOPG was higher than that of the mica system in a basic solution. Bhosle et al.[21] adsorbed purified capsular polysaccharide (fr2 ps) on Ge and Ge-oxide surfaces to characterize molecular interaction with a focus on divalent cation and pH effect (pH 3−10) on the adsorption process using attenuated total internal reflection Fourier transform infrared spectroscopy. However, these methods often need advanced molecular-level resolution to understand the underlying mechanisms fully.[22] Computational simulations, such as density functional theory (DFT) and molecular dynamic (MD), offer an alternative approach that can provide detailed insights into the interactions between individual EPS molecules and the graphite surface at the atomic scale.[23]

In recent times, scientists have been studying how proteins and biomolecules bind to graphite- and graphene-based surfaces using quantum chemical computations. Köhler et al.[24] used MDs simulations to study the initial binding of fibrinogen to mica and graphite. They found that fibrinogen bonded more strongly to the graphite surface due to better electrostatic interactions. The number of graphite layers also affects the binding. For example, Rubio-Pereda[25] studied the initial binding of bovine serum albumin (BSA) to a nanopatterned three-layer graphite substrate (G0, G3, and G5) using long MD simulations. They reported higher binding energy for BSA on a three-layer graphite system (300 kcal/mol) due to a larger contact surface area than single-layer and five-layer systems. The results show that the stepped adsorbents (G3 and G5) preferred spontaneous binding of the protein, leading to increased protein mobility, especially for the BSA-2 orientation. Despite progress made, there is a dearth of research on the interaction between a bacterium EPS and a graphite electrode. Several other works have focused on biomolecules applicable to dental science, medicine, and antimicrobial resistance rather than on electroactive bacteria surface molecules, which when effectively attached to graphite electrode surfaces can increase electron transfer and subsequent power generation while functioning as a wastewater treatment tool.

Therefore, the purpose of this study was to use DFT and MD to show that bacteria's extracellular polymeric substances (EPS) contained in their biofilm can be adsorbed on the graphite electrode and that further modifying the graphite electrode surface would increase the adsorption of the EPS. We also compared the adsorption of all three EPS models used to determine which one adsorbs best on the modified surface. This work involves evaluating how microorganisms bind to the graphite surface and assessing how surface modification, solvent environment, pH, and temperature influence the EPS binding capacity.

2. PROCESS AND COMPUTATIONAL DETAILS

2.1. DFT Studies. Calculations and simulations were performed using Material Studio software (BIOVIA Materials Studio Academic Research Suite; Product No: 5CB-LUR). We imported a graphite crystal from the materials studio library of crystals and applied the lattice parameters for graphite (a = 2.47 Å = b and c = 6.93 Å; α = 90° = β and γ = 120°). A detailed description of the crystal structure of graphite is provided in the Supporting Information. To optimize and account for the effect of exchange−correlation of the adsorbates (NAG, alginate, and D-glucose) and substrates (virgin and hydroxylated graphite), the Dmol^3 tool was used. Particularly, the generalized gradient approximation-based exchange function,[26] spin-free Perdew−Burke−Ernzerhof functional with basis set double numerical plus "d" function basis, and basis file 3.5[27] were used, coupled with the COSMOS solvation model[28] to account for the hydration. We then calculated all quantum chemical parameters (Table S1) using

https://doi.org/10.1021/acsomega.4c08032
ACS Omega 2024, 9, 48711−48720

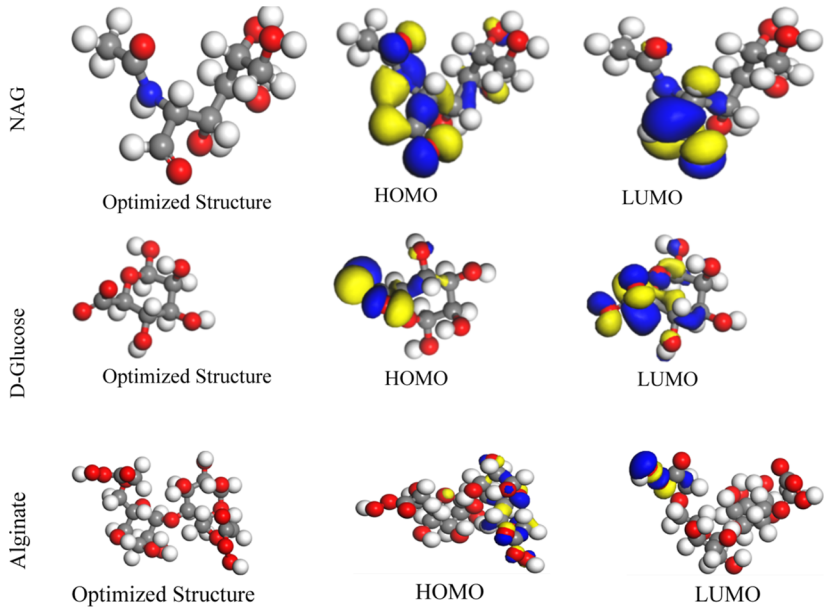

Figure 1. Electronic structures of NAG ($C_8H_{15}NO_6$), D-glucose ($C_6H_{12}O_6$), and alginate ($C_6H_{10}O_7$). Gray = C, blue = N, red = O, and white = H. Yellow and blue isosurfaces represent electron density: yellow regions represent electron loss, and blue regions represent electron build-up.

frontier molecular orbitals [highest occupied molecular orbital (HOMO) and lowest unoccupied molecular orbital (LUMO)].

The last few parameters (in Table S1) starting from the electronegativity (χ) were calculated using the energy results from the Frontier molecular orbitals, as indicated in eqs 1−7, respectively.[22,29,30]

$$\chi = -\frac{E_{HOMO} + E_{LUMO}}{2} \quad (1)$$

$$\eta = \frac{E_{LUMO} - E_{HOMO}}{2} \quad (2)$$

$$\delta = \frac{2}{E_{LUMO} - E_{HOMO}} \quad (3)$$

$$\Delta E_{back\text{-}donation} = -\frac{1}{4}\eta \quad (4)$$

$$\boldsymbol{\varepsilon} = \frac{1}{\omega} \quad (5)$$

$$\omega^- = \frac{(E_{HOMO} + 3E_{LUMO})^2}{16(E_{LUMO} - E_{HOMO})} \quad (6)$$

$$\omega^+ = \omega^- \times \frac{(E_{HOMO} + 3E_{LUMO})^2}{(3E_{HOMO} + E_{LUMO})^2} \quad (7)$$

The fraction of electrons transferred from the sorbates to the graphite surface can be calculated as follows.[31,32]

$$\Delta N_{max} = \frac{\chi}{2\eta} \quad (8)$$

The Fukui function is a useful reactivity descriptor of a molecule as it unveils a molecule's active sites for electrophilic, nucleophilic, and radical attack by other molecules.[33] eqs 9−11 can be used to study the Fukui indexes.

$$f_k(\vec{r})^+ = q_k(\boldsymbol{N} + \boldsymbol{1}) - q_k(\boldsymbol{N}) \quad (9)$$

$$f_k(\vec{r})^- = q_k(\boldsymbol{N}) - q_k(\boldsymbol{N} - \boldsymbol{1}) \quad (10)$$

$$f_k(\vec{r})^0 = \frac{1}{2}[q_k(\boldsymbol{N} - \boldsymbol{1}) - q_k(\boldsymbol{N} + \boldsymbol{1}) \quad (11)$$

where $q_k(N - 1)$, $q_k(N)$, and $q_k(N + 1)$ are the electron density at point r for the molecules with $N - 1$, N, and $N + 1$ electrons, respectively.

2.2. MDs Simulation. The adsorption locator tool of BIOVIA Materials Studio 2020 was used to construct a substrate−molecule-solvent system. A $(35\ Å)^3$ simulation box was used for simulating the interaction between the adsorbates (NAG, alginate, and D-glucose) and the adsorbent (pure graphite and hydroxylated graphite) surface. A 35 Å thick vacuum plate was introduced on the graphite (002) surface and then expanded to a supercell (7 × 7 × 7). The hydroxylated graphite surface was prepared by anchoring OH (inclined at 109.485°) to the basal plane hexagonal carbon atoms of the graphite crystals. A detailed description of the chemical characteristics of all molecules and sorbents used is presented in Table S2. For optimization of the surfaces, adsorbates, ions, and solvents, we employed the COPASS II force field with convergence tolerance energy of 2.0×10^{-5} kcal/mol and a force of 1.0×10^{-3} kcal/mol/A.[28] The force field nonbonding parameters including electrostatic cutoff distance, spline width, and buffer were set to 18.5 1 and 0.5 Å, respectively, while the bonded parameters for electrostatic and van der Waals were set to atom-based.

For the adsorption simulation, we created a solvent environment containing 250 water molecules, while 5 (H_3O^+; Cl^-) and 5 (Na^+; OH^-) ions were used to create acidic and basic environments within the solvent, respectively. Three temperatures (298, 303, and 308 K) were selected for assessing the effect of temperature change on the adsorption of the molecules. These pH and temperature conditions are crucial to the bacteria adhesion process and were therefore factored into this study. The Ewald simulation model was used for treating the long-distance electrostatic interactions, while interactions with van der Waals interactions were treated with

https://doi.org/10.1021/acsomega.4c08032
ACS Omega 2024, 9, 48711−48720

a cutoff distance of 15.5 Å and a spline width of 1.0 Å. The number of steps per cycle was 50,000/cycles for five cycles and a maximum iteration of 500. We carried out the adsorption on the selected basal surface of the graphite where we performed the initial −OH surface modification. The potential interaction energy of the adsorbates-substrate system was calculated according to eq 12.

$$E_{ads} = E_{system} - (E_{surface} + E_{molecule}) \quad (12)$$

where E_{ads} is the interaction energy between the molecules in the aqueous phase and graphite (002) surface, E_{system} is the energy of the adsorbates-substrate system, $E_{surface}$ is the energy of the individual graphite (002) surface, and $E_{molecule}$ is the energy of the molecules.

The radial distribution is useful for understanding the binding process that occurs within a solvent medium, particularly highlighting the probability of finding a molecule that is r distance away from a reference point.[34] It is calculated using eq 13.

$$g(r) = \left(\frac{n(r)}{4\pi^2 dr}\right) / \left(\frac{N_B}{V}\right) \quad (13)$$

where $n(r)$ is the average number of molecules in the area range $r - dr \leq r \leq r + dr$, r represents the distance between the adsorbate of interest and the atoms on the adsorbent surface, N_B represents the total number of molecules, and V represents the systems.

3. RESULTS AND DISCUSSION

3.1. Electronic Distribution. The optimized structures for graphite crystal (a), unmodified graphite (b), and modified graphite (c) are presented in Figure S1, while the HOMO and LUMO of the three adsorbates (NAG, D-glucose, and alginate) are shown in Figure 1.

The HOMO and LUMO structures for all of the adsorbates studied are provided in Figure 1.

The adsorption of NAG, alginate, and D-glucose on graphite (002) surface typically involves Lewis acid−base interactions, in which the graphite adsorbent and adsorbate molecules act as Lewis acid and Lewis base, respectively, and interact by a favorable overlap of the Frontier HOMO and LUMO orbitals. In this case, their electronic structures can be modeled by application of the HSAB (hard/soft acid/base) principle. Indeed, the structural and electronic properties of a molecule can be used to tune its chemical reactivity at the molecular level. A lower E_{LUMO} implies a favorable electron acceptance or electron affinity, while a high E_{HOMO} indicates the ability of a molecule to donate electrons. Table 1 gives the calculated global descriptors involved with the reactivity of NAG, D-glucose, and alginate including E_{LUMO}, E_{HOMO}, energy gap (ΔE_{gap}), softness and hardness, electronegativity, fraction of electrons transferred (ΔN), and energy change ($\Delta E_{back\text{-}donation}$).

Table 1 shows that the highest E_{HOMO} was obtained from D-glucose (−5.026 eV), followed by alginate (−6.075 eV), while the lowest E_{HOMO} was obtained from NAG (−6.123 eV). The order increases as follows: NAG < alginate < D-glucose. The result indicates that D-glucose possesses a high electron-donating capacity for donating electrons to electron-deficient centers, indicating its high potential to be a nucleophile. NAG has the lowest E_{LUMO}, indicating its ability to accept electrons and serve as a better electrophile than alginate and D-glucose, respectively. The order of electrophilicity increases as follows:

Table 1. Quantum Chemical Parameters for NAG, Alginate, and D-Glucose

parameters	NAG	D-glucose	alginate
E_{HOMO}	−6.123	−5.026	−6.075
E_{LUMO}	−2.446	−0.071	−2.316
ΔE_{gap} (eV)	3.677	4.955	3.759
I (eV)	6.123	5.026	6.075
E_a (eV)	2.446	0.071	2.316
χ (eV)	4.285	2.549	4.196
μ (eV)	−4.285	−2.549	−4.196
η (eV)	1.839	2.4775	1.880
δ (eV−1)	0.544	0.404	0.532
ω	4.992	1.311	4.683
ε	0.200	0.763	0.214
ω^+	0.229	0.066	0.217
ω^-	7.364	2.895	7.015
ΔN	1.165	0.514	1.116
$\Delta E_{back\text{-}donation}$	−0.460	−0.619	−0.470
total energy (kcal/mol)	−819.422	−760.890	−1379.034

NAG > alginate > D-glucose. The ability of a molecule to accept electrons (low E_{LUMO}) influences its adsorption properties.[35] It can be seen that NAG shows the lowest energy gap (ΔE_{gap} = 3.677 eV), indicating its potential for chemical reactivity and adsorption at the graphite (002) surface.[36] From the results, the electronegativity increases in the order: $\chi_{D\text{-}glucose} < \chi_{alginate} < \chi_{NAG}$.[37,38] NAG shows the highest electronegativity (χ_{NAG} = 4.285 eV). Differences in electronegativity values create an asymmetric distribution of electrons, giving rise to efficient dipole−dipole interaction with the substrate, thereby increasing adsorption at the graphite (002) surface.[34] Moreover, chemical hardness indicates a system's stability, and the chemical hardness increases by the order NAG < alginate < D-glucose, making D-glucose ($\eta_{D\text{-}glucose}$ = 2.4775 eV) the hardest molecule. The order of the softness for the molecules studied can be given by D-glucose < alginate < NAG. It can be reasoned that the softest and most reactive molecule is NAG (δ = 0.5439 eV^{-1}), making it more favorable for the interaction with the graphite (002) surface due to efficient electron transfer.[22]

In general, the soft−soft and hard−hard interactions depend on low hardness value and high softness value, which controls adsorption on the graphite (002) surface. $\Delta E_{back\text{-}donation} < 0$ for all molecules, hence all molecules used are energetically feasible. Since higher values of ω^+ indicate better electron-accepting ability while lower values of ω^- imply better electron-donating capacity,[39] NAG attains the best electron-accepting ability. The higher the absolute value of the fraction of electron transfer ($|\Delta N|$) gets, the higher a molecule's tendency to transfer electrons to the substrate. NAG showed the highest value of ΔN, indicating the strongest ability to transfer electrons. Therefore, all molecules studied have the potential to form either by hydrogen bonds, electrostatic bonds, or $\pi-\pi$ stacking with the −OH groups, empty p-orbital, and C=C, thus existing as Lewis bases. This behavior is crucial to the stability and operation of the microbial fuel cell since a continuous acid−base interaction motivates a continuous transfer of electrons from the bacteria to the cathode through the anode. Consequently, the performance of the MFC is expected to be stable. Research suggests that acid−base interactions favoring alkaline conditions (pH 9.0) enhance electron transfer kinetics and biofilm formation,

https://doi.org/10.1021/acsomega.4c08032
ACS Omega 2024, 9, 48711−48720

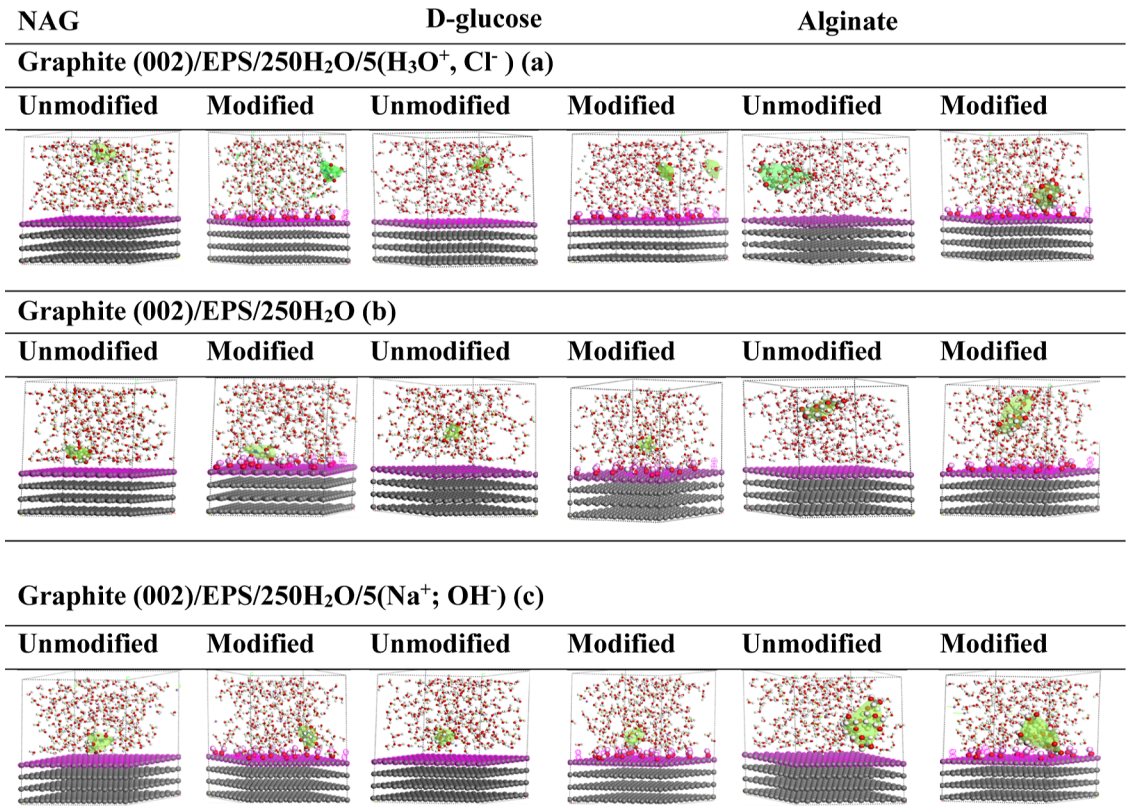

Figure 2. Adsorption equilibrium conformation of unmodified and modified graphite for all three adsorbate−adsorbent complexes (NAG, D-glucose, and alginate) in acidic (a), neutral (b), and basic (c) media.

Table 2. MDs Descriptors (in kcal/mol) of the Most Energetically Feasible Systems for Unmodified and Modified Graphite Complexes with all Three Adsorbates (NAG, D-Glucose, and Alginate)

	NAG		D-glucose		alginate	
parameters(kcal/mol)	unmodified	modified	unmodified	modified	unmodified	modified
VDW	314.560	339.910	−2847.309	327.667	342.892	352.614
$E_{electrostatic}$	−2735.231	−2735.253	−2422.393	−2472.936	−2510.192	−2535.151
E_{tot}	−2836.228	−2726.698	−2054.055	−326.552	−4834.355	−83560.058
E_{ads}	−3159.747	−3297.291	−2597.156	−2813.140	−2965.705	−3190.047
$E_{deformation}$	212.302	212.933	−4674.629	−3168.845	−109251.993	0.0000
RAE	−3325.349	−3172.639	−2955.080	−2510.192	−3561.148	−2597.156
$dE_{ads}/dNi_{molecue}$	−64.982	−53.453	−20.936	−812.592	−13.351	−3.883
$dE_{ads}/dNiH_2O$	−13.573	0.516	−152.800	−164.392	−122.576	−101.050
dE_{ads}/dNi medium	−107.222	−104.946	−95.303	−12.196	−109911.528	−121.040

resulting in higher power densities compared to neutral or acidic conditions.[40]

3.2. Mulliken Charge Distribution. The local reactivity of each adsorbate molecule was further analyzed by calculation of the Fukui indices to identify reactive regions in a molecule for electrophilic (f_k^-) and nucleophilic (f_k^+) attack.[41] Table S2 shows the calculated Fukui indices based on Mulliken.[51]

The most reactive sites for nucleophilic attack were C_{13} (0.369) for NAG, while the most preferred sites for electrophilic attack were O_5 (0.225) for NAG, O_{23} (0.066) for alginate, and O_7 (0.392) for D-glucose. Therefore, D-glucose showed the most active site for electrophilic attack, while NAG had the most preferred site for nucleophilic attack. In general, electron donation increased in the following order: NAG < alginate < D-glucose. These electron-donating sites are involved in electron transfer to the empty p-orbitals of the graphite for the formation of coordination bonds. The results from the Fukui functions agree with the quantum chemical descriptors. Overall, the DFT results indicate that all molecules are capable of adsorbing on the surface of the graphite (002) with the highest preference given to NAG due to its low energy gap and chemical stability and reactivity.

3.3. Adsorption Studies. The molecular interaction between the molecules studied (NAG, Alginate, D-glucose) and the graphite (002) surface without solvent is presented in Figure S2. Akinola et al.[42] believe that solvent molecules compete with the adsorbates for active sites on the adsorbent. This means that an adsorption will be efficient without the solvent compared to one occurring in a solvent.

The adsorptions of EPS are shown in an aqueous medium at 298, 303, and 308 K, and pH (acidic, neutral, and basic) was investigated with MDs using the Forcite and Adsorption Locator modules. MD revealed the most energetically feasible configuration of the adsorbed molecules and the adsorption

https://doi.org/10.1021/acsomega.4c08032
ACS Omega 2024, 9, 48711−48720

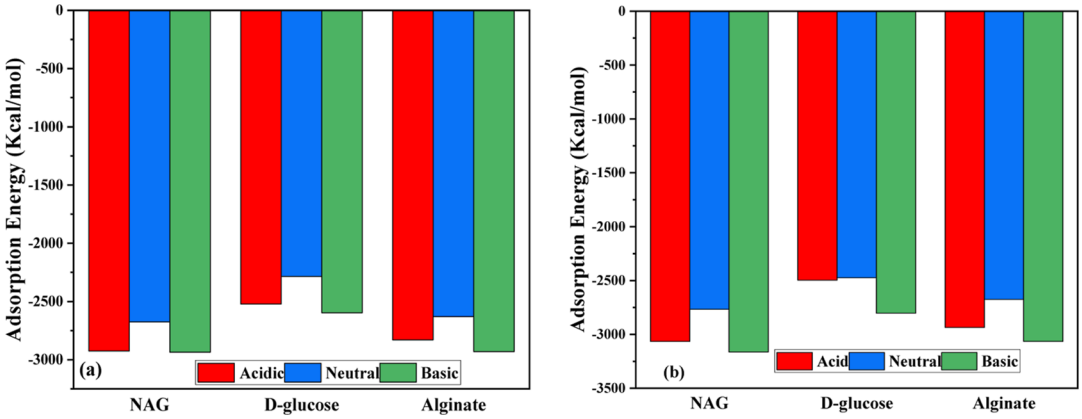

Figure 3. Effect of pH on the adsorption energy for the most stable configurations for (a) unmodified graphite and (b) modified complexes in three media.

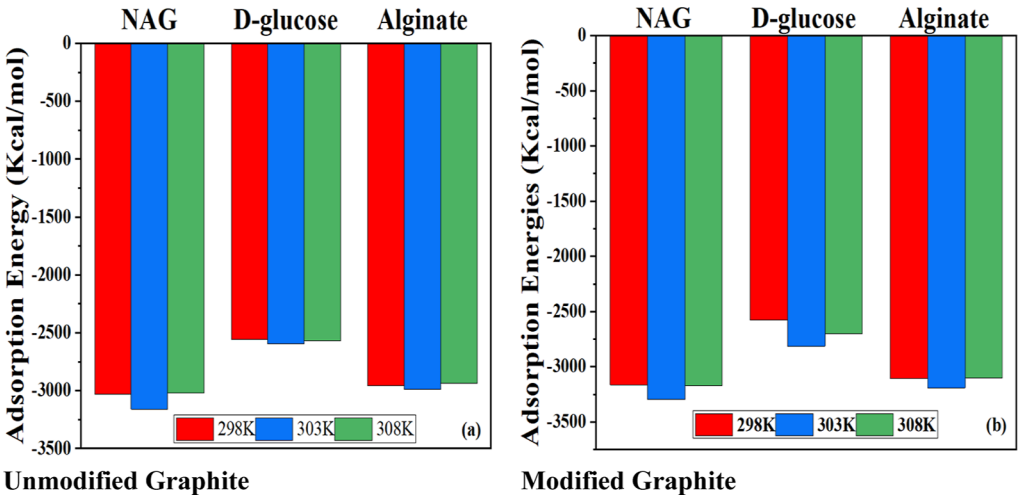

Figure 4. Effect of temperature change on the adsorption energies of the most stable configurations of NAG, D-glucose, and alginate complexes in a basic medium for unmodified (a) and modified (b).

mechanism of the adsorbate−adsorbent complex. The conformation of the adsorbate−adsorbent systems is presented for both unmodified and modified graphite complexes under various pH conditions, as shown in Figure 2. Adsorption parameters such as the binding energy, van der Waals, total energy, electrostatics, average total energies, and intermolecular energies for the sorbate−substrate system are presented in Table 2.

From Table 2, the highest van der Waals exhibited by the molecules originated from alginate (342.892) for the virgin graphite adsorption, while a much higher value from NAG (352.614) was observed for the hydroxylated graphite (002)−adsorbate system. One reason for this slightly high value for modified graphite is the additional electron-rich −OH groups present on the modified graphite surface, which increases the overall van der Waals interactions.[43] In addition, since negative values of the total energy indicate favorable adsorption, it follows that all of the molecules were favorably adsorbed on the graphite surfaces. This reasoning is confirmed by the adsorption energy, given by[22]

$$E_{ads} = (E_{sorbate} + E_{sorbent}) - E_{sys} \quad (14)$$

It can be observed that the adsorption energies for both unmodified and modified systems are all negative and increased in the following order: D-glucose < alginate < NAG, which was earlier predicted by the DFT results. This indicates the favorability of the adsorbates forming complexes with the adsorbent via chemical bonding.[43] This conclusion is parallel with a modified graphite surface due to increased H-bonding, which overcomes the activation barrier.[22] Lastly, in both unmodified and modified systems, NAG showed the highest electrostatic energy (−2735.231 and −2735.253 kcal/mol, respectively). The negative electrostatic energies for all systems indicate that adsorption occurred either by chemisorption through electron exchange or by physisorption through electrostatic interactions.[44]

3.4. Effect of pH on Adsorption. The pH is a significant factor for both biological and chemical systems. As the pH increases, the competition reduces, increasing access to the active site by the sorbate, or an extremely high pH increases the competition for active sites on the adsorbent, decreasing the adsorption energy.[45] Figure 3 shows the trend of adsorption as the pH of the adsorption cell changes from acidic to neutral to basic media.

Maximum adsorption was obtained in a basic medium for NAG, D-glucose, and alginate across all systems. These results corroborate well with experimental results, as reported by Bhosle and co-workers.[21] Moreover, the molecules studied are commonly found in bacteria including Pseudomonas, which

https://doi.org/10.1021/acsomega.4c08032
ACS Omega 2024, 9, 48711−48720

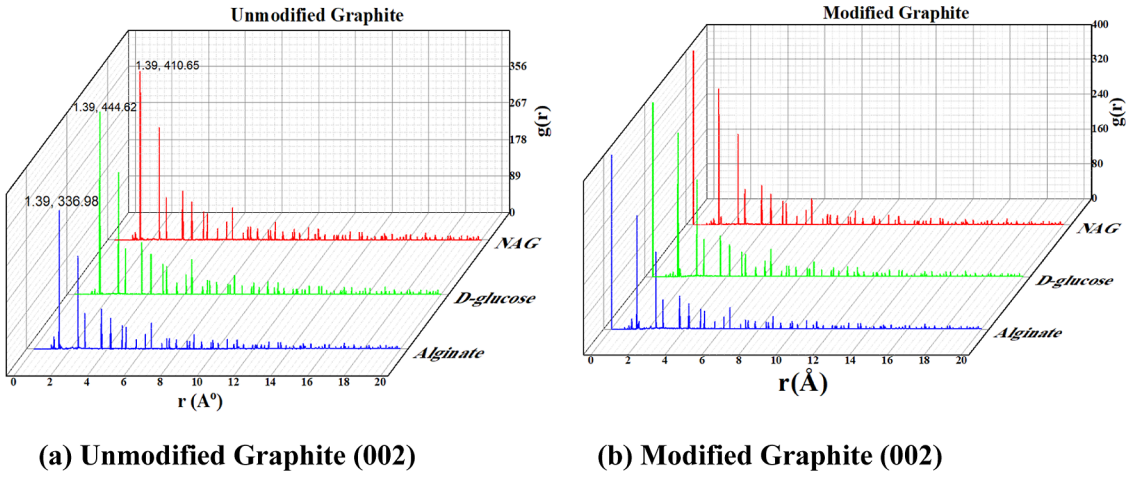

Figure 5. RDF for (a) unmodified graphite and (b) modified graphite at 30 °C in basic medium.

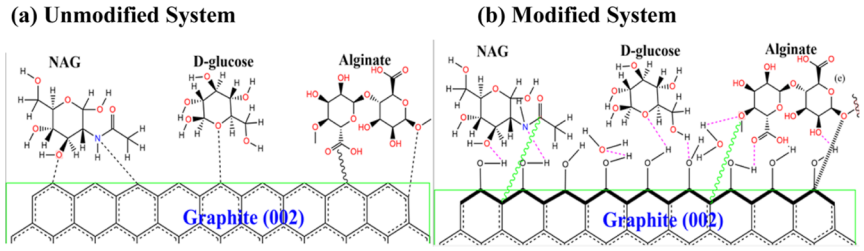

Figure 6. Adsorption mechanism for all three sorbate−sorbent complexes for (a) unmodified graphite and (b) modified graphite surfaces.

can survive or tolerate a wide range of pH including basic conditions, making this result favorable for microbial fuel cell application.

3.5. Effect of Temperature on the Adsorption Energy. Adsorption of molecules on solid substrates can be affected by temperature, particularly the filling of the local states in the bandgap.[46] The effect of temperature on adsorption−desorption equilibrium is often useful for predicting whether the adsorbate−adsorbent interaction is by chemisorption or physisorption. Although the boundary between chemisorption and physisorption in this regard is rather nebulous, some experimental validation exists, wherein a decrease in surface coverage with a temperature increase is correlated with physisorption, while the reverse is correlated with chemisorption. However, high temperatures disrupt and break the weak van der Waals bonds associated with physisorption. Figure 4 shows the effect of the temperature change on the adsorption energies for all three adsorbates.

The results show a consistent trend for all systems, wherein E_{ads} increased slightly as the temperature changed from 298 to 303 K and then dropped slightly with a further increase in temperature from 303 to 308 K. In all, temperature increases did not lead to a significant reduction in adsorption energy as usual for physisorption systems, which implies a predominance of chemisorptive interactions across all systems.[47]

3.63.6. Radial Distribution Function. The radial distribution or correlation function (RDF or CF) is useful for understanding the binding process that occurs within a solvent medium, particularly highlighting the probability of finding a molecule that is r distance away.[34] The highest peaks represent the most preferred distances the substrates are from the sorbent within the system. Figure 5 presents the RDF for all three adsorbates on unmodified and modified graphite. If r < 3.5 Å, the adsorption is said to be chemisorption.[48]

The radial distribution function (RDF) for both unmodified and modified systems indicates that the highest peaks are all less than 3.5 Å, which shows a strong chemical interaction between the sorbate and sorbent[49] having almost no variations in all pH media. Compared to the unmodified graphite, modified graphite exhibited more chemisorption, an average shift from 1.45 Å in the unmodified system to 0.00 Å in the modified system. In general, chemisorption is more favorable on the modified graphite surfaces, even though both modified and unmodified systems underwent chemisorption. Similar observations have been reported in the literature with molecular hydrogen.[50] The stability and immobility of adsorbed molecules increase with chain length, and lateral interactions between adsorbates contribute to the formation of ordered structures.[51] While the adsorbate−adsorbent interaction is guided by their proximity and therefore determines the stability and subsequent electron transfer rate, the adsorbate−adsorbate interaction is primarily mediated by graphene's π electrons within the graphite unit and can be tuned by adjusting adsorbate-graphene bonding or chemical potential.[52] It is worth noting that the preceding lines indicate that the RDF is likely inversely related to the reactivity and stability of the adsorbate−adsorbent complex, which can contribute to the long-term operation and stability of the MFC due to continuous electron transfer from attached bacteria.

4. MECHANISM OF ADSORPTION

Figure 6 shows the mechanism of adsorption for all three molecules on the unmodified and modified graphite surfaces.

NAG has an acetyl group (CH_3CO) that can participate in electrostatic interactions using its carbonyl group (C═O) and

https://doi.org/10.1021/acsomega.4c08032
ACS Omega 2024, 9, 48711−48720

lead to different interaction patterns with the graphite surface.[53] However, the amine (−NH−) and hydroxyl groups were responsible for the hydrogen bonding between the delocalized "pi" electrons and lone pairs. On the other hand, D-glucose has multiple hydroxyl (OH) groups that can participate in hydrogen bonding with surface oxygen atoms on the graphite (002) plane. This hydrogen bonding is more likely a key driver of the adsorption process, particularly in the modified system.[54] The molecule adsorbed on the graphite surface, with its hydroxyl groups facing the surface shown in the solvated systems (Figure 2) and the sugar ring lying flat shown in the nonsolvated system (Figure S2). Weak attractive forces between the negatively charged carboxylate groups on alginate and the electron-rich surface of the graphite plane affected the adsorption, irrespective of their distance apart. Finally, water molecules can compete with adsorbates for hydrogen bonding sites on the graphite surface, potentially affecting the adsorption strength and orientation. In conclusion, as evidenced by the DFT results, the primary active sites involved in the bonding are the O, N, and carbon in acetate. These findings are in agreement with the DFT results.

5. CONCLUSIONS

Modifying the graphite surface with OH functional groups enhanced the adsorption energies and subsequent electron transfer, which could improve energy production in microbial fuel cells and advance environmental remediation. The study found that all bacteria EPS used were capable of adsorbing on both unmodified and modified graphite surfaces, with NAG exhibiting the highest chemical interaction. The Fukui function results showed that the most active sites are located at O, C_{13}, and N on the adsorbates. The optimum operating conditions were in a basic medium at T = 303 K across all systems. Electrostatic interactions, hydrogen bonding, and $\pi-\pi$ stacking were the driving forces for the formation of chemical bonds between the adsorbates and adsorbents. The DFT and MD descriptors provide theoretical support for the advancement of biocompatible electrode materials in fuel cells and energy, environmental and sustainable chemistry, and computational and theoretical chemistry. These findings apply to biofouling and antifouling, dental science, clean energy production, and wastewater treatment. Further research could explore other EPS such as humic acids or uronic acid or different surface modifications such as $-NH_2$, −COOH, $-PO_3$, or a combination. Of course, there is still a need for experimental validations of these DFT results.

■ ASSOCIATED CONTENT

Data Availability Statement

All data are available in the Supporting Information for Review Only.

Supporting Information

The Supporting Information is available free of charge at https://pubs.acs.org/doi/10.1021/acsomega.4c08032.

List of all quantum chemical parameters used in the study; optimized structures for the graphite (002) substrate; adsorption of EPS on graphite in non-solvent media; and Fukui function indices for EPS molecules (PDF)

■ AUTHOR INFORMATION

Corresponding Authors

G. Plason Zuerkanah Plakar − *Federal University of Technology, Africa Centre of Excellence in Future Energies and Electrochemical Systems (ACE-FUELS), Owerri, Imo State 460114, Nigeria;* Present Address: Department of Chemistry, Cuttington University, Republic of Liberia; orcid.org/0000-0002-6003-2114; Email: plakar.plasonz@gmail.com

Emeka Emmanuel Oguzie − *Federal University of Technology, Africa Centre of Excellence in Future Energies and Electrochemical Systems (ACE-FUELS), Owerri, Imo State 460114, Nigeria;* orcid.org/0000-0003-2708-9298; Email: emekaoguzie@futo.edu.ng

Authors

Fredy Harcel Kamgang Djioko − *Federal University of Technology, Africa Centre of Excellence in Future Energies and Electrochemical Systems (ACE-FUELS), Owerri, Imo State 460114, Nigeria*

Kanayo L. Oguzie − *Federal University of Technology, Africa Centre of Excellence in Future Energies and Electrochemical Systems (ACE-FUELS), Owerri, Imo State 460114, Nigeria*

Complete contact information is available at: https://pubs.acs.org/10.1021/acsomega.4c08032

Notes

The authors declare no competing financial interest.

■ ACKNOWLEDGMENTS

The authors remain grateful to the Second Africa Higher Education Centres of Excellence for Development Impact (ACE Impact) Project, funded by the World Bank and the French Development Agency (AFD) designated P169064, IDA no. 6510 NG.

■ REFERENCES

(1) Li, S.; Cheng, C.; Thomas, A. Carbon-Based Microbial-Fuel-Cell Electrodes: From Conductive Supports to Active Catalysts. *Adv. Mater.* **2017**, *29* (8), 1602547.

(2) McCreery, R. L. Advanced Carbon Electrode Materials for Molecular Electrochemistry. *Chem. Rev.* **2008**, *108* (7), 2646−2687.

(3) Li, S.; Cheng, C.; Thomas, A. Carbon-Based Microbial-Fuel-Cell Electrodes: From Conductive Supports to Active Catalysts. *Adv. Mater.* **2017**, *29*, 1602547.

(4) Hussain, R. T.; Umar, K.; Ahmad, A.; Bhawani, S. A.; Alshammari, M. B. Conventional Electrode Materials for Microbial. In *Microbial Fuel Cells for Environmental Remediation*; Springer, 2022; pp 83−117.

(5) Dai, J.-F.; et al. Surface Properties Of Graphene: Relationship To Graphene-Polymer Composites. *Rev. Adv. Mater. Sci.* **2015**, *40*, 60.

(6) Li, C. C.; Wang, Y. J.; Du, H.; Cai, P.; Peijnenburg, W. J. G. M.; Zhou, D. M. Influence of bacterial extracellular polymeric substances on the sorption of Zn on γ-alumina: A combination of FTIR and EXAFS studies. *Environ. Pollut.* **2017**, *220*, 997−1004.

(7) Liu, H.; Li, L. Graphitic materials: Intrinsic hydrophilicity and its implications. *Mech. Lett.* **2017**, *14*, 44−50.

(8) Fan, B. B.; Wang, H. L.; Guan, L.; Chen, D. L.; Zhang, R. Ab Initio Study of Water Clusters Adsorption on Graphite Surface. *Adv. Mater. Res.* **2010**, *105−106* (106), 499−501.

(9) Picaud, S.; Collignon, B.; Hoang, P. N. M.; Rayez, J.-C. Adsorption of water molecules on partially oxidized graphite surfaces: a molecular dynamics study of the competition between OH and COOH sites. *Phys. Chem. Chem. Phys.* **2008**, *10* (46), 6998.

(10) Collignon, B.; Hoang, P. N. M.; Picaud, S.; Rayez, J. C. Ab initio study of the water adsorption on hydroxylated graphite surfaces. *Chem. Phys. Lett.* **2005**, *406* (4−6), 430−435.
(11) Gao, X.; Zhang, Y.; Li, X.; Ye, J. Novel graphite sheet used as an anodic material for high-performance microbial fuel cells. *Mater. Lett.* **2013**, *105*, 24−27.
(12) Sicard, J. F.; Vogeleer, P.; Le Bihan, G.; Olivera, Y. R.; Beaudry, F.; Jacques, M.; Harel, J. N-Acetyl-glucosamine influences the biofilm formation of Escherichia coli. *Gut Pathog.* **2018**, *10*, 26.
(13) Jain, S.; Chen, J., "Attachment and Biofilm Formation by Various Serotypes of Salmonella as Influenced by Cellulose Production and Thin Aggregative Fimbriae Biosynthesis," **2007**.*70*, 2473, 2479, ,
(14) Orgad, O.; Oren, Y.; Walker, S. L.; Herzberg, M. The role of alginate in Pseudomonas aeruginosa EPS adherence, viscoelastic properties and cell attachment. *Biofouling* **2011**, *27* (7), 787−798.
(15) Limoli, D. H.; Jones, C. J.; Wozniak, D. J. Bacterial Extracellular Polysaccharides in Biofilm Formation and Function. *Microbiol. Spectr.* **2015**, *3*, 223.
(16) Berne, C.; Ducret, A.; Hardy, G. G.; Brun, Y. V. Adhesins Involved in Attachment to Abiotic Surfaces by Gram-Negative Bacteria. *Microbiol. Spectr.* **2015**, *3*, 163.
(17) Hlady, V.; Buijs, J. Protein adsorption on solid surfaces. *Curr. Opin. Biotechnol.* **1996**, *7*, 72−77.
(18) Dash, S.; Lahiri, D.; Nag, M.; Das, D., Ray, R. R., "Probing the Surface-Attached In Vitro Microbial Biofilms with Atomic Force (AFM) and Scanning Probe Microscopy (SPM)," **2021**; pp 223−241..
(19) Wan Dagang, W. R. Z.; Bowen, J.; O'Keeffe, J.; Robbins, P. T.; Zhang, Z. Adhesion of Pseudomonas fluorescens biofilms to glass, stainless steel and cellulose. *Biotechnol. Lett.* **2016**, *38* (5), 787−792.
(20) Yang, H.; Fung, S. Y.; Pritzker, M.; Chen, P. Modification of Hydrophilic and Hydrophobic Surfaces Using an Ionic-Complementary Peptide. *PLoS One* **2007**, *2*, No. e1325.
(21) Bhosle, N.; Suci, P. A.; Baty, A. M.; Weiner, R. M., Geesey, G. G., "Influence of Divalent Cations and pH on Adsorption of a Bacterial Polysaccharide Adhesin," **1998**.*205*, 89, 96, ,
(22) Khnifira, M.; Mahsoune, A.; Belghiti, M.; Khamar, L.; Sadiq, M.; Abdennouri, M.; Barka, N. Combined DFT and MD simulation approach for the study of SO2 and CO2 adsorption on graphite (111) surface in aqueous medium. *Curr. Res. Green Sustainable Chem.* **2021**, *4*, 100085.
(23) Singh, S. K.; Chaurasia, A.; Verma, A. Basics of Density Functional Theory, Molecular Dynamics, and Monte Carlo Simulation Techniques in Materials Science. In *Coating materials: Computational aspects, applications and challenges*; Springer, 2023; pp 111−124.
(24) Köhler, S.; Schmid, F.; Settanni, G. Molecular Dynamics Simulations of the Initial Adsorption Stages of Fibrinogen on Mica and Graphite Surfaces. *Langmuir* **2015**, *31* (48), 13180−13190.
(25) Rubio-Pereda, P.; Vilhena, J. G.; Takeuchi, N.; Serena, P. A.; Pérez, R. Albumin (BSA) adsorption onto graphite stepped surfaces. *J. Chem. Phys.* **2017**, *146*, 214704.
(26) Djioko, F. H. K.; Fotsop, C. G.; Youbi, G. K.; Nwanonenyi, S. C.; Madu, C. A.; Oguzie, E. E. Unraveling the sorption mechanisms of ciprofloxacin on the surface of zeolite 4A (001) in aqueous medium by DFT and MC approaches. *Appl. Surf. Sci. Adv.* **2024**, *19*, 100542.
(27) Djioko, F. H. K.; Fotsop, C. G.; Youbi, G. K.; Nwanonenyi, S. C.; Oguzie, E. E.; Madu, C. A. Efficient removal of pharmaceutical contaminant in wastewater using low-cost zeolite 4A derived from kaolin: Experimental and theoretical studies. *Mater. Chem. Phys.* **2024**, *315*, 128994.
(28) Klamt, A.; Jonas, V.; Bürger, T., Lohrenz, J. C. W., "Refinement and Parametrization of COSMO-RS," **1998**.*102*, 5074, 5085, ,
(29) Boumya, W.; Khnifira, M.; Machrouhi, A.; Abdennouri, M.; Sadiq, M.; Achak, M.; Serdaroğlu, G.; Kaya, S.; Şimşek, S.; Barka, N. Adsorption of Eriochrome Black T on the chitin surface: Experimental study, DFT calculations and molecular dynamics simulation. *J. Mol. Liq.* **2021**, *331*, 115706.
(30) Oguzie, E. E.; Njoku, D. I.; Chidebere, M. A.; Ogukwe, C. E.; Onuoha, G. N.; Oguzie, K. L.; Ibisi, N. Characterization and experimental and computational assessment of Kola nitida extract for corrosion inhibiting efficacy. *Ind. Eng. Chem. Res.* **2014**, *53* (14), 5886−5894.
(31) Bratsch, S. G. Electronegativity equalization with Pauling units. *J. Chem. Educ.* **1984**, *61* (7), 588.
(32) Oguike, R. S.; Kolo, A. M.; Shibdawa, A. M.; Gyenna, H. A. Density Functional Theory of Mild Steel Corrosion in Acidic Media Using Dyes as Inhibitor: Adsorption onto Fe(110) from Gas Phase. *ISRN Phys. Chem.* **2013**, *2013*, 1−9.
(33) Zaklika, J.; Hładyszowski, J.; Ordon, P.; Komorowski, L. From the Electron Density Gradient to the Quantitative Reactivity Indicators: Local Softness and the Fukui Function. *ACS Omega* **2022**, *7* (9), 7745−7758.
(34) Sneha, P.; Doss, C. G. P. Molecular Dynamics. *Adv. Protein Chem. Struct. Biol.* **2016**, *102*, 181−224.
(35) Khalil, N. Quantum chemical approach of corrosion inhibition. *Electrochim. Acta* **2003**, *48* (18), 2635−2640.
(36) Njoku, D. I.; Li, Y.; Lgaz, H.; Oguzie, E. E. Dispersive adsorption of Xylopia aethiopica constituents on carbon steel in acid-chloride medium: A combined experimental and theoretical approach. *J. Mol. Liq.* **2018**, *249*, 371−388.
(37) Ghashghaee, M.; Ghambarian, M. Initiation of heterogeneous Schrock-type Mo and W oxide metathesis catalysts: A quantum thermochemical study. *Comput. Mater. Sci.* **2018**, *155*, 197−208.
(38) Obot, I. B.; Obi-Egbedi, N. O.; Eseola, A. O. Anticorrosion potential of 2-mesityl-1H-imidazo[4,5-f] [1,10]phenanthroline on mild steel in sulfuric acid solution: Experimental and theoretical study. *Ind. Eng. Chem. Res.* **2011**, *50* (4), 2098−2110.
(39) Singh, A.; Ansari, K. R.; Banerjee, P.; Murmu, M.; Quraishi, M. A.; Lin, Y. Corrosion inhibition behavior of piperidinium based ionic liquids on Q235 steel in hydrochloric acid solution: Experimental, density functional theory and molecular dynamics study. *Colloids Surf. A Physicochem. Eng. Asp.* **2021**, *623*, 126708.
(40) Yuan, Y.; Zhao, B.; Zhou, S.; Zhong, S.; Zhuang, L. Electrocatalytic activity of anodic biofilm responses to pH changes in microbial fuel cells. *Bioresour. Technol.* **2011**, *102* (13), 6887−6891.
(41) Nwanonenyi, S. C.; Obasi, H. C.; Chukwujike, I. C.; Chidiebere, M. A.; Oguzie, E. E. Inhibition of Carbon Steel Corrosion in 1 M H2SO4 Using Soy Polymer and Polyvinylpyrrolidone. *Chem. Afr.* **2019**, *2* (2), 277−289.
(42) Akinola, J.; Campbell, C. T.; Singh, N. Effects of Solvents on Adsorption Energies: a General Bond-Additivity Model. *J. Phys. Chem. C* **2021**, *125*, 24371−24380.
(43) Han, Z.; Sun, L.; Chu, Y.; Wang, J.; Wei, C.; Jiang, Q.; Han, C.; Yan, H.; Song, X. States of graphene oxide and surface functional groups amid adsorption of dyes and heavy metal ions. *Chin. J. Chem. Eng.* **2023**, *63*, 197−208.
(44) Djioko, F. H. K.; Fotsop, C. G.; Youbi, G. K.; Nwanonenyi, S. C.; Madu, C. A.; Oguzie, E. E. Unraveling the sorption mechanisms of ciprofloxacin on the surface of zeolite 4A (001) in aqueous medium by DFT and MC approaches. *Appl. Surf. Sci. Adv.* **2024**, *19*, 100542.
(45) Li, R.; Li, H.; Xu, S.; Liu, J. Theoretical investigation of the effect of OH− ions on O2 adsorption on low-index Pt surfaces in alkaline solution. *Appl. Surf. Sci.* **2015**, *351*, 853−861.
(46) Davydov, S. Y. On the role of temperature in the problem of adsorption on graphene. *Technical Physics* **2016**, *61* (7), 1106−1108.
(47) Berger, A. H.; Bhown, A. S. Comparing physisorption and chemisorption solid sorbents for use separating CO2 from flue gas using temperature swing adsorption. *Energy Procedia* **2011**, *4*, 562−567.
(48) Wood, B. C.; Bhide, S. Y.; Dutta, D.; Kandagal, V. S.; Pathak, A. D.; Punnathanam, S. N.; Ayappa, K. G.; Narasimhan, S. Methane and carbon dioxide adsorption on edge-functionalized graphene: A comparative DFT study. *J. Chem. Phys.* **2012**, *137*, 054702.
(49) Wood, B. C.; Bhide, S. Y.; Dutta, D.; Kandagal, V. S.; Pathak, A. D.; Punnathanam, S. N.; Ayappa, K. G.; Narasimhan, S. Methane and

https://doi.org/10.1021/acsomega.4c08032
ACS Omega 2024, 9, 48711−48720

carbon dioxide adsorption on edge-functionalized graphene: A comparative DFT study. *J. Chem. Phys.* **2012**, *137*, 054702.
(50) Volpe, M.; Cleri, F. Chemisorption of atomic hydrogen in graphite and carbon nanotubes. *Surf. Sci.* **2003**, *544* (1), 24−34.
(51) Zhao, Y.; Chen, Y. Nano-TiO 2 enhanced photofermentative hydrogen produced from the dark fermentation liquid of waste activated sludge. *Environ. Sci. Technol.* **2011**, *45* (19), 8589−8595.
(52) Solenov, D.; Junkermeier, C.; Reinecke, T. L.; Velizhanin, K. A. Tunable Adsorbate-Adsorbate Interactions on Graphene. *Phys. Rev. Lett.* **2013**, *111* (11), 115502.
(53) Zhong, Y.; Bauer, B. A.; Patel, S. Solvation properties ofN-acetyl-β-glucosamine: Molecular dynamics study incorporating electrostatic polarization. *J. Comput. Chem.* **2011**, *32* (16), 3339−3353.
(54) Yin, Q.; Si, L.; Wang, R.; Zhao, Z.; Li, H.; Wen, Z. DFT study on the effect of functional groups of carbonaceous surface on ammonium adsorption from water. *Chemosphere* **2022**, *287*, 132294.

https://doi.org/10.1021/acsomega.4c08032
ACS Omega 2024, 9, 48711−48720